*J. Fluid Mech.* (1980), *vol.* 98, *part* 2, *pp.* 285–297
*Printed in Great Britain*



# On the Mach reflexion of a solitary wave

By W. K. MELVILLE

Institute of Geophysics and Planetary Physics, University of California, San Diego, La Jolla, California 92093

(Received 12 April 1979)

Miles' (1977*b*) model of the Mach reflexion of a solitary wave by a vertical wall is tested by laboratory experiments. The model over-predicts the measured run-up at the wall, and no evidence of the predicted maximum was found. The measurements provide support for the predicted critical angle of incidence at which Mach reflexion is replaced by regular reflexion. It is shown that mass and energy conservation determine the length of the reflected wave in Miles' model and that this is not consistent with momentum conservation in the neighbourhood of the end point of the reflected wave. It is suggested that the discrepancy between the measurements and the model may result from this failure of the model.

## 1. Introduction

Miles (1977*b*) has recently conjectured that the Mach reflexion† of a solitary wave at a rigid wall may be described by the resonant interaction of three Boussinesq solitary waves. Earlier observations and experiments (Perroud 1957; Chen 1961; Wiegel 1964*a*, *b*) had revealed that regular reflexion of a solitary wave is impossible for sufficiently small angles of incidence and is replaced by Mach reflexion. The apex of the incident and reflected waves then moves away from the wall and is joined to it by the Mach stem.

Although the experiments of these workers display qualitative agreement with Miles' model, they do not confirm the more important of his predictions: the angle of incidence at which Mach reflexion gives over to regular reflexion, and the run-up at the wall. The primary purpose of the present paper is to report an experimental study of Mach reflexion and to examine the validity of Miles' model.

### 1.1. *Miles' model*

A solitary wave of free-surface displacement $\epsilon d\eta$ in water of quiescent depth $d$ is given by

$$\eta = k^2 \operatorname{sech}^2 \theta + O(\epsilon), \tag{1.1}$$

where $\theta = \mathbf{k}.\mathbf{x} - \omega t + \theta_0$,

$$\mathbf{k} = k\{\cos\psi, \sin\psi\}, \quad \omega \equiv kc = k\{1 + \tfrac{1}{2}k^2\epsilon + O(\epsilon^2)\} \tag{1.2}$$

are the phase, wavenumber and circular frequency, $c$ is the wave speed, $\theta_0$ is a phase constant, $\mathbf{x} \equiv \{x, y\}$ is the co-ordinate vector in a horizontal plane, and $\epsilon$ is a small

† The phenomenon is named after the geometrically similar reflexion of a gasdynamic shock at a corner.

0022-1120/80/4445-8990 $02.00 

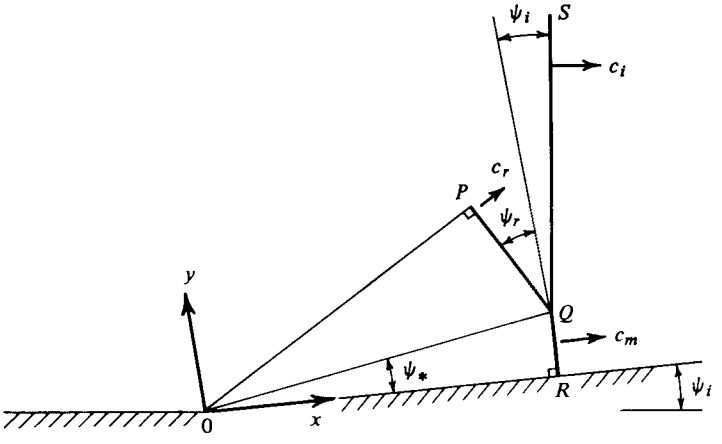


FIGURE 1. The Mach-reflexion pattern, where $SQ$ is the incident wave, $PQ$ the reflected wave, and $QR$ the Mach stem.

parameter. The Mach reflexion is depicted in figure 1, wherein the subscripts $i$, $r$ and $m$ refer to the incident wave, the reflected wave, and the Mach stem, respectively. Miles concluded that an asymptotically stationary resonant reflexion pattern is attained wherein

$$\{k_i, k_r, k_m\} = \{1, k, 1+k\}, \tag{1.3a}$$

and the angles subtended at the normal to the wall are given by

$$(\psi_i, \psi_r, \psi_m) = (3\epsilon)^{\frac{1}{2}}\{k, 1, 0\}, \tag{1.3b}$$

$k = \psi_i/(3\epsilon)^{\frac{1}{2}}$, and the dimensionless amplitude of the incident wave, $k_i^2$, is taken to be unity. The apex of the incident and reflected waves moves away from the wall at a constant angle, $\psi_*$, with speed $c_*$ where

$$\psi_* = (\tfrac{1}{3}\epsilon)^{\frac{1}{2}}(1-k), \quad c_* = 1 + \tfrac{2}{3}\epsilon(1+k+k^2). \tag{1.4a,b}$$

It follows from (1.3) that the amplitude of the reflected wave decreases from 1 to 0 as $\psi_i$ decreases from $(3\epsilon)^{\frac{1}{2}}$ to 0, whilst the stem angle $\psi_*$ increases from 0 to $(\frac{1}{3}\epsilon)^{\frac{1}{2}}$, i.e. the Mach stem disappears at the critical angle

$$\psi_i = \psi_c \equiv (3\epsilon)^{\frac{1}{2}}. \tag{1.5}$$

Miles combined (1.3) with his earlier treatment of obliquely interacting solitary waves (Miles 1977$a$) and concluded that the run-up at the inclined wall, $\alpha_w d$, is given by

$$\frac{\alpha_w}{\alpha_i} = \begin{cases} 4[1+(1-k^{-2})^{\frac{1}{2}}]^{-1} & (\psi_i^2 > 3\epsilon), \quad (1.6a) \\ (1+k)^2 & (\psi_i^2 < 3\epsilon), \quad (1.6b) \end{cases}$$

where $\alpha_i d$ is the amplitude of the incident wave.†

### 1.2. *Perroud's measurements*

Perroud's (1957; see also Wiegel 1964$a$, $b$) measurements are perhaps the only data that are available for the Mach reflexion of a solitary wave at a rigid vertical wall. The majority of measurements were made in a ripple tank of depth 4 cm for $\alpha_i$ in the range 0·08–0·38. Surface displacements were made with resistance wave gauges (of

† The surface displacement is given by $\alpha d$, with the local maximum denoted by the corresponding subscript on $\alpha$: $\alpha_i = \epsilon$.

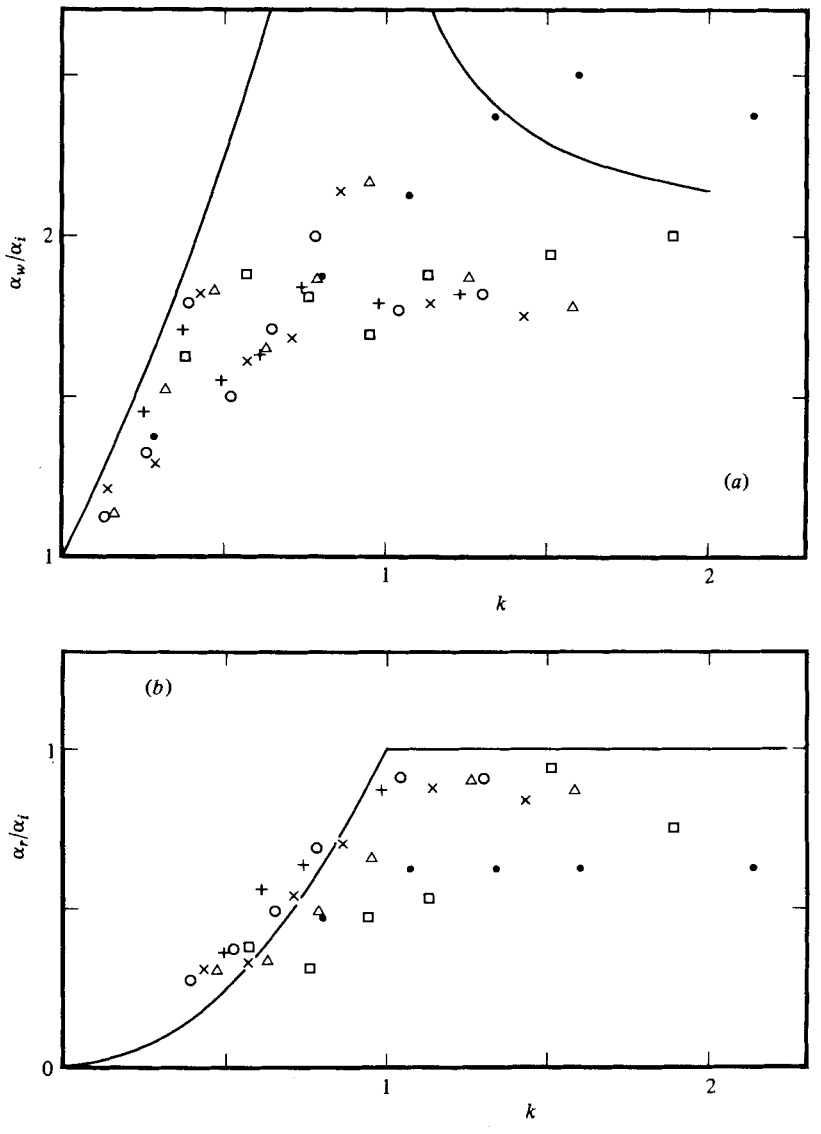


FIGURE 2. Perroud's (1957) measurements of (*a*) the run-up at the wall, and (*b*) the amplitude of the reflected wave, replotted together with Miles' (1977*b*) predictions (——). $\alpha_i$ values: ●, 0·08; □, 0·16; △, 0·23; ×, 0·28; ○, 0·34; +, 0·38.

wire diameter 0·16 cm) and were stated to have an error of 'less than ± 10 % . . . for wave heights not too small'.† Perroud found that the critical angle separating Mach and regular reflexion '. . . seems to be 45°', and that the height of the incident wave had little influence on the reflexion pattern: $\psi_r$ and $\psi_*$ were sensibly independent of $\alpha_i$. His measurements of the run-up at the wall and the amplitude of the reflected wave are shown in figures 2 (*a*) and 2 (*b*) respectively. These figures show fair agreement with Miles' model for $k \ll 1$, but the predicted extremum in $\alpha_w$ is not evident at $k = 1$.

† The fact that the ratio of wire diameter to incident wave amplitude was in the range 0·1–0·5 would suggest that this error estimate may be optimistic.

However, Perroud's experiments showed evidence of capillary effects, and wave breaking was evident in a significant number of cases.

Perroud's experiments do not provide a definitive test of Miles' model and the experiments reported here were designed to overcome the problems of scale evident in Perroud's results.

## 2. Experiments

The experiments were carried out in a wave basin 18·3 m long and 6·2 m wide, with water of 0·2 and 0·3 m depth. An extensive survey of the concrete basin floor with a theodolite showed it to be horizontal to within $\pm$ 0·5 cm, giving a corresponding error in the depth of the water. The longer side walls of the basin were made of asbestos board and were carefully aligned and sealed. The inclined wall was made of asbestos board hinged to the side wall at a distance of 4·2 m from the northern end of the basin. The inclined wall could be rotated about the vertical hinge to give the required angle of incidence. The bottom of the inclined wall was sealed with a flexible gasket compressed between its lower edge and the floor of the basin.

Solitary waves were generated by a vertical bulkhead that spanned the northern end of the basin and was actuated by a servo-controlled hydraulic system. The horizontal displacement of the bulkhead responded linearly to the input voltage, which was the analogue of the horizontal displacement of the corresponding fluid particle. This was computed digitally for each water depth and wave amplitude and was recorded on magnetic tape for subsequent play-back. The surface displacement was measured with resistance wave gauges having a resolution of $\pm$ 0·02 cm. The method of solitary-wave generation, and the wave gauges, have been described in greater detail by Chang, Melville & Miles (1979).

The incident wave was measured at two stations on a line parallel to the incident wave crest, intersecting the vertex of the inclined wall and the side wall. The effects of capillarity in the immediate vicinity of the wall were avoided by making measurements at no less than 2 cm from the wall. This distance is typically two orders of magnitude less than the horizontal scale of the reflexion pattern, and no significant difference was evident between the wave amplitudes measured at this position and at a distance of 5 cm from the wall.

The experimental procedure was as follows. The water surface was skimmed continuously overnight and the depth checked and adjusted immediately prior to beginning the experiment. The wave gauges were statically calibrated in 1 cm steps and the gain of the wave generator checked and adjusted to give the required wave amplitude. The series of measurements along and normal to the wall were conducted separately. In the former case two gauges were used. The solitary wave was generated a number of times, with both gauges being moved between runs, giving measurements at one metre intervals along the wall. In the latter case three gauges were used suspended from a steel beam normal to the wall. One gauge was fixed 5 cm from the wall, while the other two were moved between runs. The time between runs was sufficient to ensure a quiescent surface (but see § 3.2). Each series of measurements lasted two to four hours, after which time the gauges were recalibrated. Typically, the difference in the two calibrations was $\pm$ 0·04 cm, and no correction for this drift was made. The surface displacement was recovered by linear interpolation of the

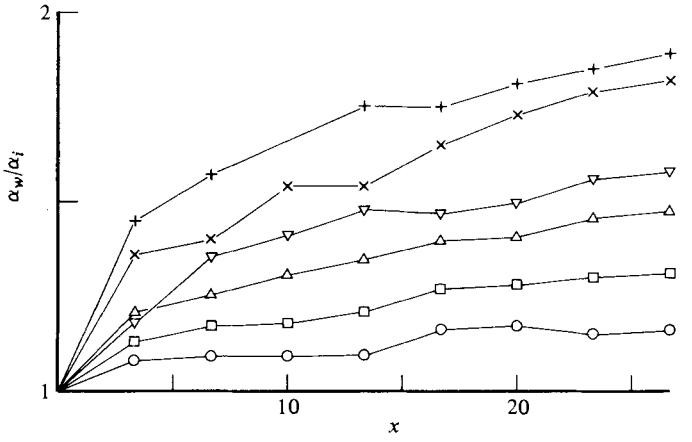


FIGURE 3. Measured run-up at the wall as a function of $x$ for $\alpha_i = 0{\cdot}1$ and for $\psi_i$ values: ○, 10°; □, 15°; △, 20°; ▽, 25°; ×, 30°; +, 35°.

calibrations. The analogue output of the wave gauges was sampled digitally at 100 or 167 Hz and recorded for subsequent processing. For each time series the mean of the first second of data was used as the datum from which the surface elevation was computed.

A solitary wave of dimensionless amplitude $\alpha$ has a characteristic length proportional to $\alpha^{-\frac{1}{2}}$. The dimensions of the available wave basin then impose a considerable constraint on the lowest wave amplitude that may be studied. On the other hand, in order to avoid wave breaking at the wall the incident wave must be relatively small. Further, the basin dimensions impose a restraint on the maximum angle of incidence that may be obtained while still retaining a useful length of inclined wall. Within these constraints the experimental conditions were, $h = 20$, 30 cm, $\alpha_i = 0{\cdot}1$, $0{\cdot}15$, $\psi_i = 0°$–$45°$. Note that $\psi_c = 31°23'$, $38°26'$ for $\alpha_i = 0{\cdot}1$, $0{\cdot}15$, respectively.

## 3. Results

In all the results presented here the position of the measurements will be given by the orthogonal co-ordinates $(x, y)$ non-dimensionalized with respect to the quiescent water depth, $h$. The inclined wall having its vertex at the origin defines the $x$ axis (see figure 1). The unit of time is $(h/g)^{\frac{1}{2}}$, the time taken for a linear wave to travel a horizontal distance equivalent to one depth. Where applicable, the results will be presented in terms of either $\psi_i$ or the normalized variable $k$, according to whichever better correlates the data.

### 3.1. *Run-up at the wall*

The run-up at the wall was measured in the range $0 < x \leqslant 26{\cdot}7$ with $\alpha_i = 0{\cdot}1$, $0{\cdot}15$ in a depth of $h = 30$ cm. A limited series of measurements were carried out at $x = 24$, 30 with $\alpha_i = 0{\cdot}1$ in a depth of 20 cm. Figure 3 shows the wave amplitude at the wall plotted as $\alpha_w/\alpha_i$ *vs.* $x$ for $\alpha_i = 0{\cdot}1$ and $\psi_i$ in the range $0 < \psi_i \leqslant 35°$ $(0 < k \leqslant 1{\cdot}16)$. These data all show an initial rapid increase in $\alpha_w$ with 50 % of the final increment typically occurring in the first five depths along the wall. Within this region there appears to be significant scatter in the measurements at the larger angles. (This was

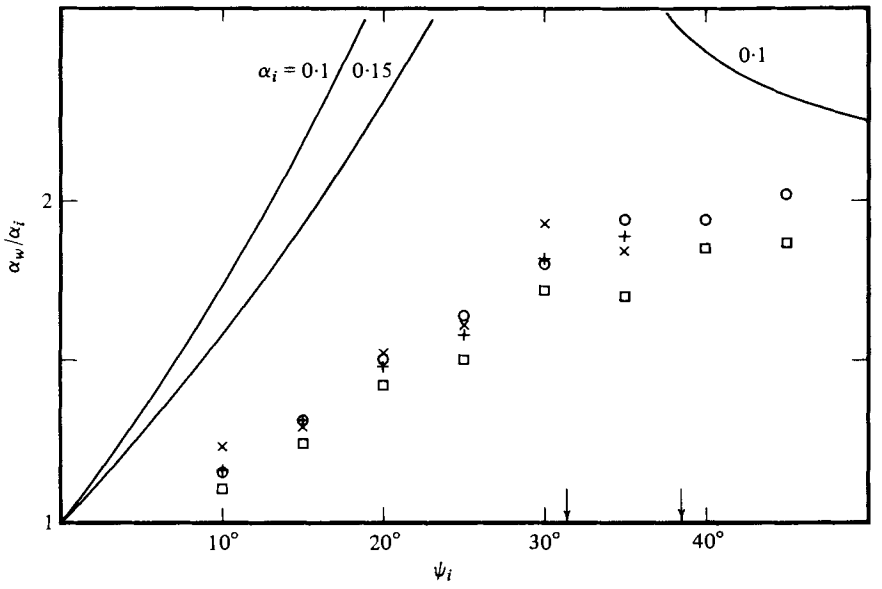


FIGURE 4. Measured run-up at the wall as a function of $\psi_i$. For $h = 30$ cm, $x = 26{\cdot}7$: +, $\alpha_i = 0{\cdot}1$; ×, $\alpha_i = 0{\cdot}15$. For $h = 20$ cm, $\alpha_i = 0{\cdot}1$: ○, $x = 24$; □, $x = 30$. The solid lines are Miles' (1977*b*) predictions for $\alpha_i = 0{\cdot}1$, $0{\cdot}15$, and the arrows indicate the corresponding predictions of the critical angle at $\psi_i = 31°23'$ and $38°26'$, respectively.

originally thought to be due to the discontinuity of slope at the wall, but attempts to remove this corner with a smooth transition showed no significant change in the measurements.) This is followed by a much slower increase in the run-up. The run-up appears to have attained an equilibrium value for the smaller angles of incidence ($\psi_i \leqslant 15°$) within the range of the measurements, but that at the larger angles still shows some growth, albeit small, at the largest values of $x$ attainable.

In figure 4 we have plotted $\alpha_w/\alpha_i$ *vs.* $\psi_i$ at $x = 26{\cdot}7$ for $h = 30$ cm, $\alpha_i = 0{\cdot}1$, $0{\cdot}15$, along with the measurements at $x = 24$, 30 for $h = 20$ cm, $\alpha_i = 0{\cdot}1$. The measurements show a monotonic increase in the run-up towards the linear result of $\alpha_w/\alpha_i = 2$. The agreement with Miles' model is poor over the range of $\psi_i$ measured. Indeed it appears that Perroud's results show somewhat better agreement (cf. figure 2*a*).

Figure 5 shows the surface displacement at $x = 16{\cdot}7$ for $\alpha_i = 0{\cdot}15$. The curves are monotonic, with those for smaller $\psi_i$ displaying a sensibly uniform plateau next to the wall. This corresponds to the Mach stem. However, the transition from the incident wave to the Mach stem is comparable to the length of the plateau, permitting no clear demarcation of the two regions.

### 3.2. *The critical angle*

In the absence of the predicted maxima in $\alpha_w$ it was not possible to measure directly the critical angle, in consequence of which it became necessary to resort to indirect means. In the Mach-reflexion pattern the crest of the Mach stem is normal to the wall, whereas the crest of the incident wave subtends an angle $\psi_i$ to the normal. The locus of the crest of the incident wave in a $(y, t)$ diagram is a straight line whose intercept on the $y$ axis is a measure of the length of the Mach stem. If the Mach stem

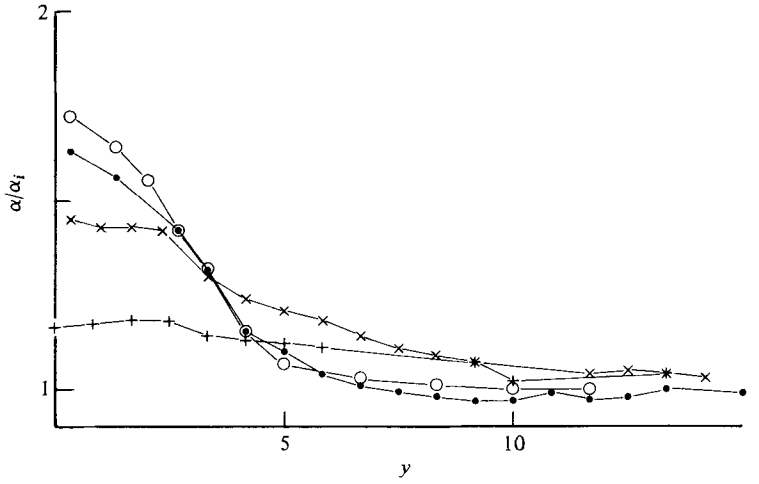


FIGURE 5. Measured surface displacement as a function of $y$ for $\alpha_i = 0{\cdot}15$ at $x = 16{\cdot}7$. $\psi_i$ values: +, 10°; ×, 20°; ●, 30°; ○ 35°.

were straight over its whole length and of uniform height and if the fluid were able to sustain discontinuities this length would be uniquely determined; however, the Mach stem may be slightly curved and the transition to the incident wave is continuous and smooth (figure 5). These real effects may lead to some ambiguity in defining the length of the Mach stem, but the differences between the intercept measure and the other readily conceivable measures are likely to be minor.

The intercept method, requiring as it does the measurement of the time between two waves crossing the normal, introduces two problems: one conceptual, and one practical. The first involves the different shapes of the Mach-stem and the incident wave (see § 3.4 below). Is the appropriate time that between maxima, the centres of mass, or some other measure of effective wave position? The second problem is that of noise. If one chooses to measure the time between maxima then even very small noise levels can lead to significant errors. The extensive use of absorbing barriers was precluded by the nature of the experiment and resulted in rather long settling times for the basin. Further, the large scale of the basin made it difficult to prevent draughts in the laboratory from generating surface waves. Both sources of noise were evident.

We resolved both the conceptual and practical problem by using a correlation technique to define the elapsed time. The correlation function between two records $\eta_i(t)$, $\eta_j(t)$ is defined by

$$R_{ij}(\tau;T) = \sum_{t=t_1}^{t_1+T} \eta_i(t)\,\eta_j(t+\tau). \tag{3.1}$$

The elapsed time between waves crossing the normal is then given by $\tau_*$, where $R_{ij}(\tau_*;T)$ is the maximum of $R_{ij}$. The length of the window was chosen to be much longer than the period of the noise but shorter than a characteristic time of the waves. Tests of 24 pairs of time series with $T/\Delta t = 32, 40, 64, 80, 100$, where $\Delta t$ is the sampling interval, showed that the mean of the maximum difference in $\tau_*$ was $\Delta t$, with a standard deviation of $\Delta t$. $T$ was set to $64\Delta t$ for all subsequent data analysis.

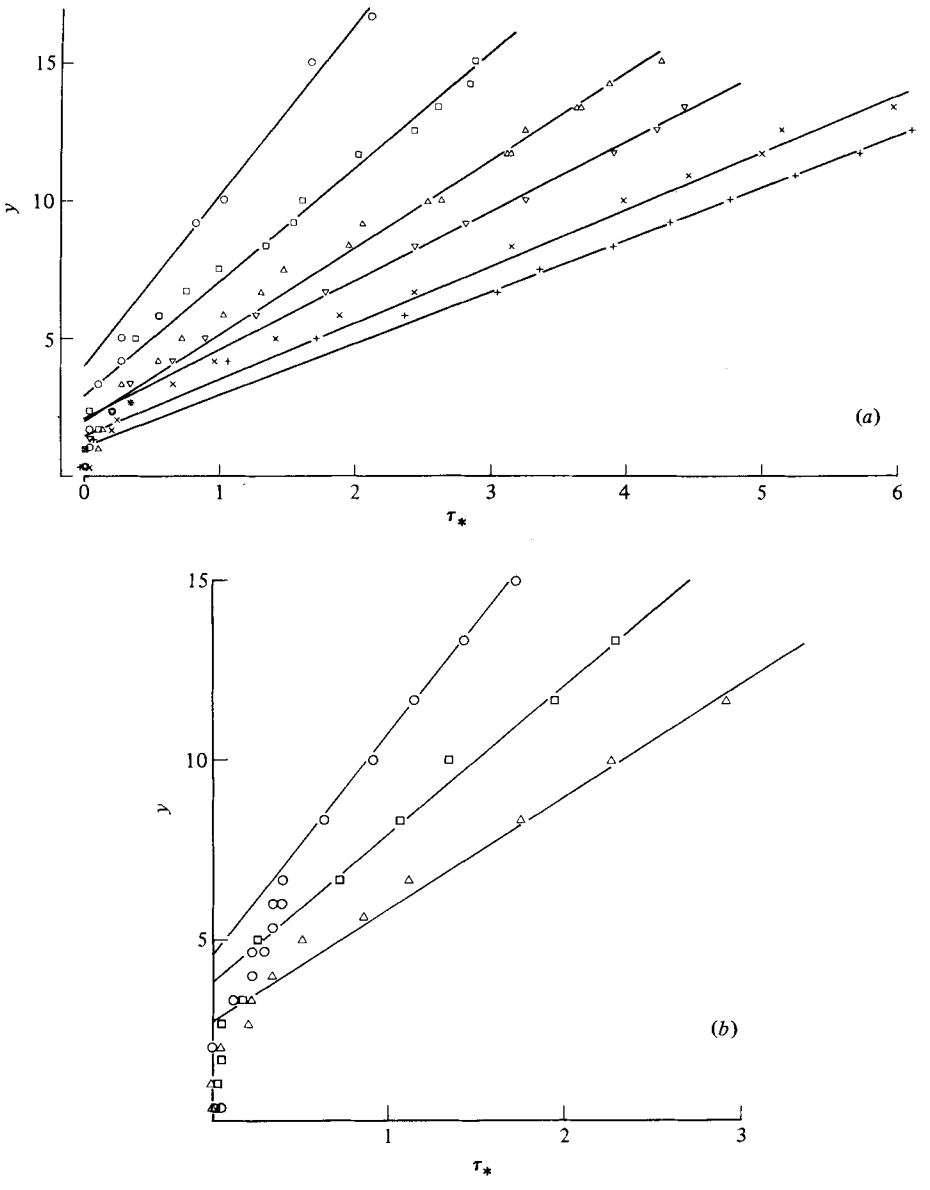


FIGURE 6. Reconstruction of the reflexion pattern from the measured elapsed time, $\tau_*$, between the wave passing at the wall and at wave gauges displaced a distance $y$ normal to the wall (see § 3.2), $\alpha_i = 0{\cdot}15$. (*a*) $x = 16{\cdot}7$. (*b*) $x = 23{\cdot}3$. $\psi_i$ values: ○, 10°; □, 15°; △, 20°; ▽, 25°; ×, 30°; +, 35°.

Figure 6(*a*, *b*) shows the $(y, \tau_*)$ diagrams for $\alpha_i = 0{\cdot}15$ at $x = 16{\cdot}7$ and $23{\cdot}3$, respectively. The slope of the locus of the incident wave in these diagrams is

$$dy/dt_* = c_i \sec \psi_i.$$

Both $c_i$ and $\psi_i$ were measured and the slope computed. The solid lines in figure 6 have the computed slope, and intercepts on the $y$ axis which bisect the range of intercepts defined by the data and the measured slope. These intercepts were then

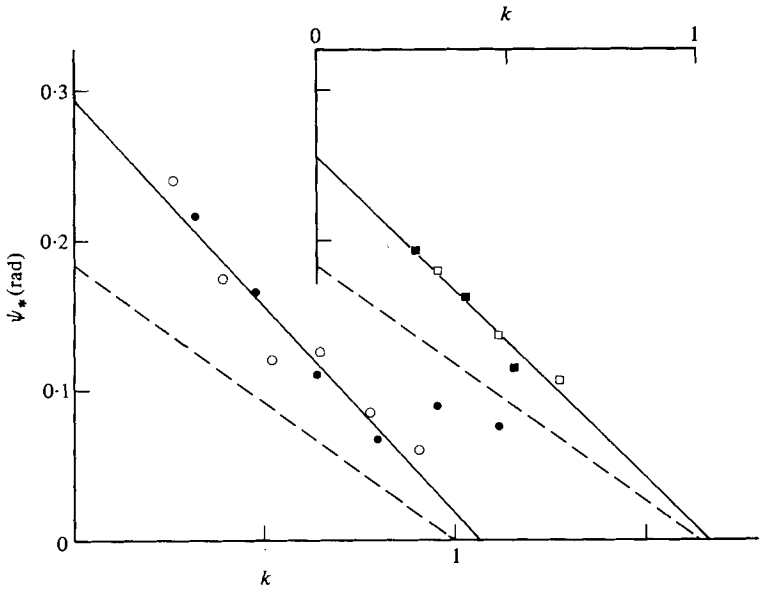


FIGURE 7. $\psi_*$ (see figure 1) determined from an extrapolation of the results depicted in figure 6 and plotted against $k$ (see § 1) for $x = 16{\cdot}7$: ●, $\alpha_i = 0{\cdot}1$; ○, $\alpha_i = 0{\cdot}15$. $x = 23{\cdot}3$: ■, $\alpha_i = 0{\cdot}1$; □, $\alpha_i = 0{\cdot}15$. The solid lines are the linear least square fits to the data. The broken lines represent Miles' (1977*b*) prediction. The intercepts of the experimental curves on the $k$ axis are at $k = 1{\cdot}07$ and $1{\cdot}03$, for $x = 16{\cdot}7$ and $23{\cdot}3$, respectively.

used to compute $\psi_*$ (cf. figure 1), the angle subtended by the Mach stem at the origin, and the results are shown in figure 7 where they are plotted against $k$. Also shown are Miles' predictions. The linear behaviour predicted by Miles is evident in the measurements, except perhaps in the neighbourhood of $k = 1$ where the measured $\psi_*$ for $x = 16{\cdot}7$, $\alpha_i = 0{\cdot}1$ are still finite. (These points support Perroud's finding that a small Mach stem still persisted at his measured critical angle.) Neglecting these two points and making linear least-square fits to the data gives intercepts on the $k$ axis at $k = 1{\cdot}07$ and $1{\cdot}03$, for data taken at $x = 16{\cdot}7$ and $23{\cdot}3$, respectively. This agreement with Miles' model is perhaps better than one might have hoped for as the results are obtained through a double extrapolation of the measurements. Nevertheless, the error is most unlikely to be as much as 50 % which is what would be required to agree with Perroud's result: $\psi_c \approx 45°$. One further feature of figure 6 is the evident decrease in the intercept on the $\psi_*$ axis with an increase in $x$. This suggests that the reflexion pattern may still be evolving at the largest value of $x$ attainable in the experiment.†

### 3.3. *The reflected wave*

The reflected wave amplitude was determined by measuring the second local maximum of the time series; the first corresponded to either the incident wave or the Mach stem. The relatively small amplitudes of the reflected wave, at least for the smaller angles of incidence, result in considerable uncertainty in the data, which are plotted

† Computing linear least-square fits to the data according to $\alpha_i$, rather than $x$ as is done in figure 7, results in intercepts on the $k$ axis at $k = 1{\cdot}01$ and $1{\cdot}05$, for $\alpha_i = 0{\cdot}1$ and $0{\cdot}15$, respectively. These results suggest that if the reflexion pattern is still evolving it is doing so very slowly.

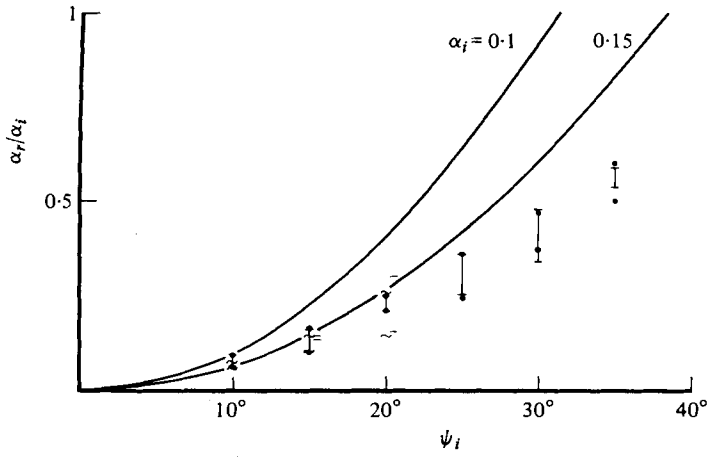


FIGURE 8. Measured reflected wave amplitudes versus $\psi_i$. For $x = 16{\cdot}7$: I, $\alpha_i = 0{\cdot}1$; ⋮, $\alpha_i = 0{\cdot}15$. For $x = 23{\cdot}3$: ⁻, $\alpha_i = 0{\cdot}1$; ≃, $\alpha_i = 0{\cdot}15$. The solid curves are Miles' (1977*b*) predictions. There was some evidence of $\alpha_r$ varying along the wave and the bars denote the range of $\alpha_r$. The symbol ⁻ has been offset for clarity.

along with Miles' predictions in figure 8. For small $\psi_i$ the agreement with the predictions is fair; however, it is clear that the data are better correlated by $\psi_i$ than by $k$.

It proved impossible to obtain a reliable measure of $\psi_r$ from the time series; however, the measurements did show that $PQ$, the length of the reflected wave, was greater than that required by Miles' model (see § 4.1).

### 3.4. *Wave profiles*

Figure 9(*a*) shows a montage of surface elevation along the normal $x = 16{\cdot}7$ for $\alpha_i = 0{\cdot}15, \psi_i = 20°$. The top profile is the furthest from the wall and shows the incident wave followed by the reflected wave. Moving towards the wall, the incident and reflected waves converge and evolve into the Mach stem. Figure 9(*b*) shows the upper and lower plots of figure 9(*a*) along with the corresponding Boussinesq profiles. The incident wave agrees very well with the Boussinesq profile except in the neighbourhood of the tail. The reflected wave is considerably different. It is not certain whether the dimensions of the basin permitted the evolution of the reflected wave to its final form, and this may account for some of the discrepancy. The Mach stem agrees moderately well with the Boussinesq profile over most of its length but consistently displays a following depression. Remarkably, this depression maintains its integrity and does not appear to result in a dispersive tail. Perroud also found this depression in his measurements.

## 4. Mass, energy and momentum

The discrepancy between Miles' model and the experimental measurements is much greater than can be accounted for by experimental error or failure of the reflexion pattern to reach the required asymptotic state. We have found some discrepancy between the measured and the corresponding Boussinesq profiles, but this too does

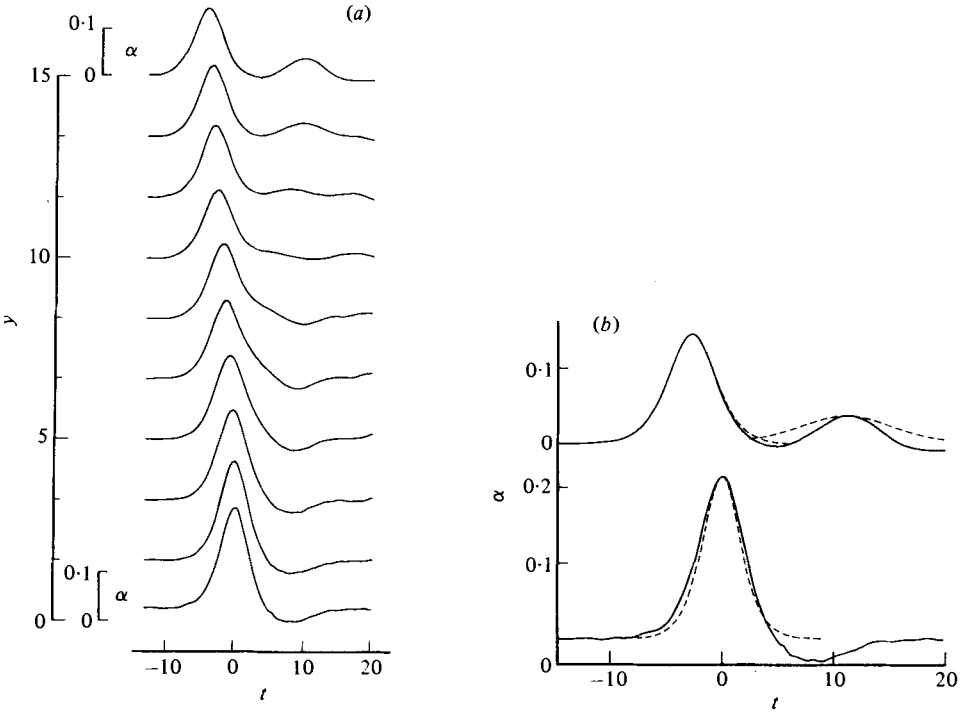


FIGURE 9. (*a*) Measured surface profiles, $\alpha$ *vs.* $t$, for $\alpha_i = 0{\cdot}15$ at $x = 16{\cdot}7$. The scale on the extreme left is the position at which the profile was measured, and the smaller inset scale is that of the surface elevation. (*b*) The upper and lower plots of (*a*), at $y = 15$ and 0·33, respectively, along with the Boussinesq profiles (– – –) corresponding to the wave amplitudes. Note that the reflected wave is much narrower than a Boussinesq solitary wave.

not appear to be sufficient to account for the large discrepancy between the measured and predicted run-up (cf. figure 4).

It is shown here that the global conservation of mass and energy along with Miles' model determines the length of the reflected wave ($PQ$ in figure 1), but that this constraint leads to a violation of momentum conservation in the neighbourhood of $P$. In § 5 it is suggested that these results may account for the discrepancies.

### 4.1. *Conservation of mass and energy*

Referring to figure 1, the increment in length per unit distance travelled by the incident wave in the $x_*$ direction is $l_i$, $l_r$, $l_m$ for the incident wave, the reflected wave and the Mach stem, respectively. Let $m_i$, $m_r$, $m_m$ be the mass per unit length of the corresponding waves and $e_i$, $e_r$, $e_m$ be the corresponding energies. From (1.3*a*) and the properties of the Boussinesq solitary wave it follows that

$$(m_i, m_r, m_m) \propto \alpha_i^{\frac{1}{2}}(1, k, 1+k), \tag{4.1a}$$

$$(e_i, e_r, e_m) \propto \alpha_i^{\frac{3}{2}}(1, k^3, \{1+k\}^3), \tag{4.1b}$$

where $\alpha_i \ll 1$, $k = O(1)$.

It is readily seen from figure 1 that, with error factors of $1 + O(\alpha_i)$,

$$l_i = -\sin(\psi_i + \psi_*) = -(\alpha_i/3)^{\frac{1}{2}}(1+2k) \tag{4.2}$$

and

$$l_m = \sin\psi_* = (\alpha_i/3)^{\frac{1}{2}}(1-k). \tag{4.3}$$

Conservation of mass requires that

$$m_i l_i + m_r l_r + m_m l_m = 0, \tag{4.4}$$

which with (4.2) and (4.3) gives the incremental length of the reflected wave:

$$l_r = (\alpha_i/3)^{\frac{1}{2}}(k+2). \tag{4.5}$$

It is readily shown that conservation of energy,

$$e_i l_i + e_r l_r + e_m l_m = 0, \tag{4.6}$$

leads to the same expression for $l_r$.

### 4.2. *Conservation of momentum*

It may be shown that equation (4.5) along with the other properties of the model imply that mass and energy are conserved if the reflected wave is terminated by the ray passing through the vertex, normal to the reflected wave. Miles (personal communication) has shown that, to within the same order of error, such a configuration is consistent with global momentum conservation. However, a global balance of momentum is a relatively weak test of the model.

The end point of the reflected wave $P$ moves with constant velocity $\mathbf{c}_r$. Consider the dynamics in a frame fixed on $P$. It is readily seen that, in order to satisfy Euler's equations and balance the pressure gradient across $P$ parallel to $PQ$, the fluid must be accelerated in the direction $\overrightarrow{QP}$. However, local mass conservation along with the constraint that the reflected wave is a Boussinesq solitary wave implies that the depth-averaged velocity component along the $PQ$ axis is zero. The model then is not consistent with momentum conservation in the neighbourhood of $P$.

## 5. Discussion

The present experiments along with those of Perroud (1957) cast considerable doubt on the use of Miles' model to describe Mach reflexion at a rigid wall.

The largest discrepancy between the model and the measurements is in the run-up at the wall. The measurements are neither extensive enough nor accurate enough to resolve the disposition of the mass carried by the Mach stem in Miles' model; nevertheless, the problem with momentum conservation elucidated in § 4 suggests a plausible explanation. We have shown that together, the hypothesis of the reflected wave being of Boussinesq form, and the resulting trajectory of the end point $P$, are not consistent with momentum conservation. If the end point $P$ has a velocity component parallel to the crest while retaining the Boussinesq wave, the end point is a source/sink of mass. This is not physically possible. If, however, the fluid in the reflected wave has a velocity component parallel to its crest then mass conservation may be satisfied. There would then be a mass flux along $\overleftarrow{PQ}$ supplied by either the incident wave or the Mach stem. A mass flux out of the Mach stem would be consistent with a reduced amplitude at the wall.

These conjectures are consistent with the observation that the length $PQ$ of the reflected wave is greater than that required for Miles' model to conserve mass and energy.

In the absence of the predicted extremum in the run-up, the method of measuring the critical-angle is not very accurate, requiring two extrapolations of the data. However, it does support Miles' prediction that $\psi_c = (3\alpha_i)^{\frac{1}{2}}$, and casts doubt on Perroud's conclusion that $\psi_c \approx 45°$.

The ray theory of solitary wave reflexion at a concave corner (Miles 1977*c*) appears to support the prediction of the run-up by the dynamical model (Miles 1977*b*). Moreover, ray-theory neglects entirely the reflected wave and thus may appear to cast some doubt on the importance attached here to the reflected wave. However, in the former model the Mach stem is still of finite length at the critical angle, carrying the mass and energy that in the latter model appears in the reflected wave. The two models then are not consistent in the neighbourhood of $k = 1$, where, due to the small length of the Mach stem, a small change in the disposition of mass may result in a large change in $\alpha_w$.

It should be stressed that our conclusions regarding the applicability of Miles' resonant interaction model to Mach reflexion at a wall do not imply that the resonant interaction solution is generally invalid. However, the resonant interaction solution is only recovered for $\alpha_i \downarrow 0$, and the boundary condition of zero transverse velocity at the inclined wall is only satisfied asymptotically as $c_* t \to \infty$. This latter constraint is consistent with the solution applying to the interaction between three waves of sensibly infinite extent (see Miles 1977*b*, table 2 and figure 3). This presents some difficulty in the context of Mach reflexion at a rigid wall for which $l_m \downarrow 0$ as $k \uparrow 1$. In addition, the resonant interaction solution does not satisfy the condition at infinity in the direction of the reflected wave, $\eta \sim o(1)$, (i.e. the reflected wave terminates in quiescent fluid); satisfying instead the asymptotic limit $\eta \sim \eta_r$, where $\eta_r = O(1)$.

I am grateful to Professor Miles for suggesting and supporting this study and for stimulating discussions on the Mach-reflexion problem. I wish to thank my colleagues at the Hydraulics Laboratory, Scripps Institution of Oceanography, for their help in conducting the experiments. This work was supported by the Physical Oceanography Division, National Science Foundation (NSF Grant OCE77-24005).

## REFERENCES

CHANG, P., MELVILLE, W. K. & MILES, J. W. 1979 On the evolution of a solitary wave in a gradually varying channel. *J. Fluid Mech.* **95**, 401–414.

CHEN, T. C. 1961 Experimental study on the solitary wave reflexion along a straight sloped wall at oblique angle of incidence. *U.S. Beach Erosion Board Tech. Memo.* no. 124.

MILES, J. W. 1977*a* Obliquely interacting solitary waves. *J. Fluid Mech.* **79**, 157–169.

MILES, J. W. 1977*b* Resonantly interacting solitary waves. *J. Fluid Mech.* **79**, 171–179.

MILES, J. W. 1977*c* Diffraction of solitary waves. *Z. angew. Math. Phys.* **28**, 889–902.

PERROUD, P. H. 1957 The solitary wave reflection along a straight vertical wall at oblique incidence. Ph.D. thesis, University of California, Berkeley.

WIEGEL, R. L. 1964*a* *Oceanographical Engineering*. Englewood Cliffs, New Jersey: Prentice-Hall.

WIEGEL, R. L. 1964*b* Water wave equivalent of Mach reflection. *Proc. 9th Conf. Coastal Engng A.S.C.E.*, cha. 6, pp. 82–102. American Society of Civil Engineers.